Direct imaging of molecules in polydiacetylene single crystals

P. H. J. Yeung and R. J. Young
Department of Materials, Queen Mary College, Mile End Road, London E1 4NS, UK
(Received 4 April 1985; revised 24 July 1985)

High resolution electron microscopy (h.r.e.m.) has been applied to a substituted polydiacetylene, poly(1,6-di(*N*-carbazolyl)-2,4-hexadiyne). Lattice images of crystal planes with spacing of less than 0.5 nm have been obtained from fibrous crystals produced by solid-state polymerization with the polymer chains perpendicular to the electron beam. Using a different preparation method, lamellar crystals can be grown with the polymer chains parallel to the electron beam. Such an orientation has enabled direct imaging of the polymer molecules viewed along the chain axis. The background noise in the experimentally obtained molecular image was filtered using a digital computer and the enhanced image contained a regular pattern of dark patches in the shape of dumb-bells. The image was compared with computer simulated images and this has confirmed the dumb-bells to be polydiacetylene molecules viewed along their chain axes to a resolution of better than 0.4 nm.

(Keywords: polydiacetylenes; high-resolution electron microscopy; lattice images; molecular images; polymer crystals)

INTRODUCTION

The application of high-resolution electron microscopy (h.r.e.m.) to the study of the crystal structure of various materials has become very common in recent years. With the resolution power of modern transmission electron microscopes (t.e.m.), scientists have been able to analyse the crystal structures of metals on the atomic level[1]. Most of the studies have been carried out successfully on metals[1,2] and oxides[3] due to their high resistance to damage from electron irradiation during t.e.m. examination. Studies of organic molecules[4,5] and polymers[6,7] are, however, more difficult due to their extreme sensitivity to electron irradiation compared with metals. Their low resistance to radiation damage in the electron beam has severely limited the resolution that can be attained. The radiation resistivity of certain organic molecules such as copper phthalocyanine can be improved by chlorination, as was demonstrated by Uyeda *et al.*[8,9] The chlorinated crystals are 30 times more stable than the unchlorinated samples under the electron beam. The use of chlorination, combined with the use of high voltage electron microscope (h.v.e.m.) to reduce radiation damage even further, has allowed molecular images of copper phthalocyanine crystals to be obtained successfully[8,9].

As far as polymeric materials are concerned, until recently only one-dimensional lattice images of a few crystalline polymers had been obtained[6,10,11]. It is only recently that molecular images of poly(*p*-xylylene) single crystal have been obtained using h.v.e.m.[12,13] This was the first time that the molecular chains of a polymer had been imaged, and the images were subsequently used to study the crystal structure of the polymer[13].

This present study is concerned with the application of h.r.e.m. to a relatively new polydiacetylene, poly(1,6-di(*N*-carbazolyl)-2,4-hexadiyne), (polyDCHD). The formula of the monomer is

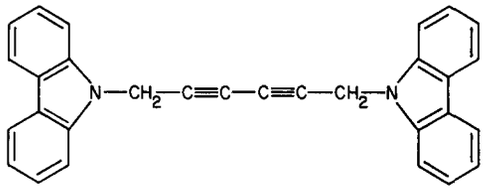

The single-crystal monomers can be polymerized in the solid-state by high-energy irradiation or thermal annealing[14,15] to form highly perfect single-crystal fibres. The polymer is monoclinic ($P2_1/c$) with $a=1.740$ nm, $b=1.287$ nm, $c=4.91$ nm and $\gamma=108.3°$. (The structure has been indexed unconventionally such that the polymer chain direction is parallel to *c*.)

In their study of radiation damage in polyDCHD, Read and Young[16] found that the polymer is considerably more beam resistant than many other polymers and is up to 40 times more beam resistant than poly(*p*-xylyene). This suggests that the molecules of polyDCHD should also be capable of being imaged if the crystals are viewed in a suitable orientation. In fact, lattice images of polyDCHD with the chains lying normal to the electron beam (side-on) have already been obtained[16,17] and the crystals have been found to have a high degree of molecular alignment and internal perfection. It has been pointed out by Read and Young[16] that the only orientation of the crystal in which the full molecular images could be revealed is with the molecular chains aligned parallel to the electron beam. Since their lattice images were obtained from crystals lying with their chains perpendicular to the electron beam, attempts to resolve molecular images were unsuccessful.

In the present study, polyDCHD has been prepared with a different crystal orientation. The crystals were grown with the polymer chains approximately

0032-3861/86/020202-09$03.00

perpendicular to the substrate (end-on). Such orientation allows the diffraction of electrons from planes parallel to the chain direction and full molecular images of polyDCHD to be obtained.

SPECIMEN PREPARATION

Side-on DCHD crystals

DCHD monomer was dissolved in boiling xylene to a concentration of 0.001 M. The solution was then filtered to remove any traces of impurities and polymer, which are insoluble in the solvent. A droplet of the monomer solution was then applied to a standard 3 mm carbon-coated electron microscope copper grid held in air at room temperature. After the solvent had evaporated, long ribbon lamellar DCHD crystals were obtained on the e.m. grid[18] and the grid was irradiated by electrons in the t.e.m. for solid-state polymerization to take place in the crystals[19].

End-on DCHD crystals

DCHD monomer was dissolved in dimethyl formamide (DMF) at room temperature to a concentration of 0.001 M. DCHD crystals were grown on a carbon-coated grid in a similar way as that of the side-on crystals except that the copper grid was placed in an air oven at 100°C. As soon as the solvent had evaporated, the grid was removed from the oven, and the crystals were subjected to solid-state polymerization in the microscope. Using this preparation method, a large number of small end-on lamellar crystals were found scattered all over the e.m. grid together with some long ribbon lamellar crystals.

HIGH RESOLUTION ELECTRON MICROSCOPY

The microscope used in this work was a JEOL (JEM) 200CX (side entry goniometer) operated at 200 kV. The high-resolution pole piece (SHP) with spherical aberration constant (C_s) value of 2 mm was used. Scherzer focus[20] for the microscope operated at 200 kV with the SHP pole piece $= -83.4$ nm. A condenser aperture of 300 μm was employed with a small beam size (spot size 3) and low beam intensity so as to minimize radiation damage of the crystals during examination.

The quality of a high-resolution image is affected by many factors such as:

(i) resolution power of the microscope,
(ii) radiation stability of the crystal under examination,
(iii) instability of the electron lenses,
(iv) vibrations,
(v) astigmatism of the objective lens
(vi) specimen drift, and
(vii) specimen thickness, etc.

Every precaution must therefore be taken to carry out the procedures necessary to overcome these potential problems encountered in recording the high-resolution images[20]. The astigmatism correction was initially carried out using a perforated carbon film in which an image was obtained of uniform width of bright Fresnel fringe around a hole magnified at about 100 000 times. Further astigmatism correction was achieved using standard specimen such as graphitized carbon black magnified to 650 000 times. The fine controls of the stigmators were adjusted until lattice images of 0.34 nm spacing were seen in all directions.

The specimen chamber of the microscope was kept cool by filling the anticontamination dewar with liquid nitrogen every 30 min. The image focusing technique was similar to that used by Read and Young[16]. The beam current was turned off while a film plate was advanced to the recording position. In this way, unnecessary beam damage to the crystal could be minimized. Image recording was not carried out for 1 min, to minimize specimen drift and allow the vibration due to film advance to settle. In order to reduce the noise in the recorded images, high-speed fine grain X-ray film such as Kodak Industrex CX was employed. The magnification was calibrated using the 0.903 nm lattice spacing of asbestos.

IMAGE ENHANCEMENT

In order to record the structural image of beam-sensitive materials at high magnifications, care must be taken not to damage the material before a useful and informative image can be recorded. This means that the total electron dosage given to the material from the moment of examination to the end of the recording should be much less than the critical exposure level[21]. A minimum exposure technique has been developed for use with biological materials[22] and organic molecules[4,5,8]. Although this technique reduces radiation damage of the material, it may give rise to the problem that background noise (due to film graininess and structure in the carbon supporting film) in the micrograph may be comparable to the structural details under observation. Sometimes the noise may even obscure the structural information in the image and it is therefore essential that the noise is filtered by some means.

Image enhancement is normally carried out using an optical filtering technique[4,23,24]. This involves setting up a laser optical bench[23] and obtaining an optical diffraction pattern from the region of the micrograph where structural image is present. A mask with appropriately located fine holes is placed in the diffraction plane to collect the diffracted beams from the periodic image of the micrograph. An image is then reconstructed by these diffracted beams, which will then reveal the periodic structure of the material without the presence of the background noise.

Another image enhancement technique was used by Fryer[5], involving spatial averaging of the image using a photographic enlarger. This technique has a major disadvantage, because great care must be taken in the random movement of the photographic paper to the exact position of each periodic unit. Failure to do so will result in an image showing the preferred direction of movement of the paper and this will render the image erroneous.

In the present study, enhancement of the molecular images of polyDCHD was effected, using a digital video framestore system (at the Dept. of Metallurgy and Science of Materials, University of Oxford)[25]. A high-resolution image micrograph magnified at about one million times was placed in front of a video camera and the image was projected onto a TV screen. The image was then digitized using a DEC mini-computer and a diffraction pattern of the image was then obtained by the computer taking a Fourier transform of the image. The aperture was electronically defined around each diffraction spot. The

image was then reformed by the computer, projected onto a TV screen and then photographed with a 35 mm camera.

RESULTS AND DISCUSSION

Lattice images of polyDCHD with molecules in the plane of the crystal

A high-resolution bright field (BF) electron micrograph of a polyDCHD crystal lying with its chains parallel to the crystal edges and normal to the electron beam is shown in *Figure 1a*. The selected area diffraction pattern (SADP) taken from the crystal (*Figure 1b*) can be seen to contain *hk*0 spots only. All the other diffraction spots were found to decay more rapidly in the beam[16]. The doubly-exposed area defines the size of the objective aperture used to select the diffraction spots in order to form the image. The corresponding *d*-spacing of the first *hk*0 diffraction spot was measured to be 1.29 ± 0.05 nm, which is close to the *d*-spacing of (010) plane (1.22 nm).

From the micrograph, lattice fringes can be seen running parallel to the edge of the crystal, which is also parallel to the chain direction of the polymer. The lattice images are similar to those obtained by Read and Young[16,17], in which no disorder can be seen along the fringes, which are perfectly straight and uniformly spaced. The spacing of the lattice fringes was measured directly from the image to be 1.31 ± 0.05 nm, which corresponds to the interplanar spacing of (010) planes and is close to that measured from the SADP. It can be noticed that this value

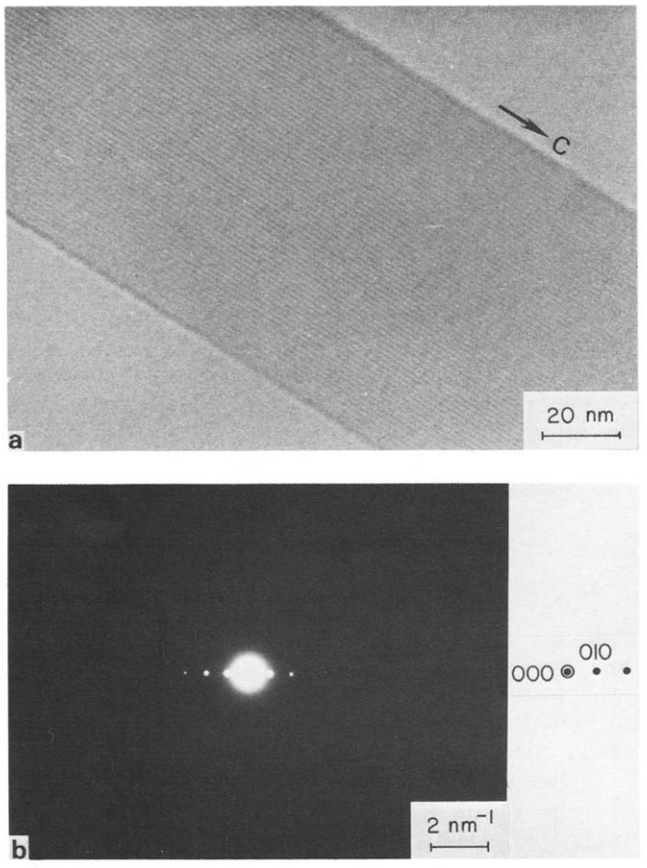

Figure 1 (a) (010) lattice image of a polyDCHD crystal lying with the chains parallel to the substrate. The spacing between the fringes was found to be 1.31 ± 0.05 nm. (b) SADP of the crystal in *Figure 1a*

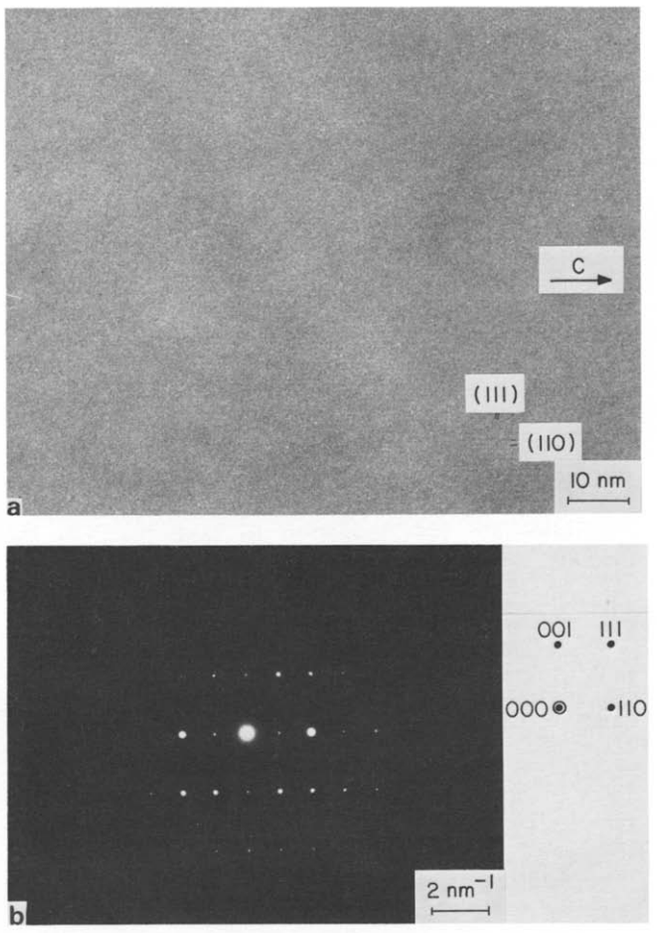

Figure 2 (a) High-resolution lattice image of a side-on polyDCHD crystal. The (110) lattice fringes can be seen running parallel to the chain direction. The (111) fringes can, however, be just seen. (b) SADP of crystal in *Figure 2a*. The beam direction corresponds to $[1\bar{1}0]$

is slightly higher than the value of (010) plane spacing (1.22 nm) measured using X-rays[26]. Similar mismatch between the measured and true (*hk*0) lattice spacings was also found by Read and Young[16]. It was thought that the change in lattice spacings was due to a small amount of crosslinking as a result of radiation damage[27].

Despite the fact that the lattice images in *Figure 1a* show perfect lattice order in the (010) plane of the polymer, details of the location and shape of individual molecules cannot be revealed. Attempts have been made to obtain high-resolution images of polyDCHD crystals with the molecules in the plane of the crystal with the images contributed by not only the equatorial diffracted beams but also azimuthal diffracted beams. Such an image is shown in *Figure 2a*. The SADP (*Figure 2b*) taken from the crystal corresponds to a beam direction of $[1\bar{1}0]$. There are about 38 diffraction spots in the pattern and all of them were used to form the high-resolution image of the crystal. From the BF micrograph widely-spaced fringes can be seen running parallel to the chain direction (as indicated by *c*). These fringes have a measured lattice spacing of 0.84 ± 0.05 nm, which corresponds to (110) planes (0.862 nm). There are also other lattice fringes which are relatively faint in contrast and narrowly spaced. These fringes are seen running at an angle to the (110) fringes. Because these fringes are very narrow and faint in contrast, an accurate measurement of their spacing is difficult to achieve. It has been estimated that these fringes have a spacing of approximately 0.46 nm, make an angle

of about 60° with the (110) fringes and so correspond to (111) planes.

Lattice fringes from other (*hkl*) planes may also be imaged but, as can be seen in the micrograph, the background noise is too dominant for any structural image, if any, to be revealed. However, even the present image was contributed by more than the minimum required diffracted beams (20) necessary to produce a structural image[20]; the image is not expected to contain information about the detailed shape of the individual molecules. As pointed out by Read and Young[16], the only direction that a detailed structural image of polyDCHD molecules may be obtained is with the beam parallel to the chain direction, when the side groups are seen superimposed. In this case, the beam direction is clearly not parallel to *c*, and so structural images of the molecules are not expected. Nonetheless, it has been shown that, with careful operation of the t.e.m., lattice images of planes other than the (*hk*0) type can be obtained. The image in *Figure 2a* is different from the one-dimensional lattice images shown in *Figure 1a* and those reported by Read and Young[16,17] in that it is a two-dimensional crossed-lattice image that has not been reported before. This is the first time that lattice images of (*hkl*) planes in polyDCHD have been obtained, even though they appeared to be more sensitive to radiation damage than the (*hk*0) planes[16]. The success of imaging the (*hkl*) lattice planes may largely be due to the use of a higher accelerating voltage and a more careful t.e.m. operation technique.

PolyDCHD single crystals with the molecules perpendicular to the plane of supporting film

Figure 3a shows a BF micrograph of a typical polyDCHD microscopic lamellar single crystal that has a morphology different from the ordinary solution crystallized ones, which are in the form of long ribbon lamellae. The crystal prepared by rapid evaporation of monomer solution at 100°C is much smaller in size than the long flat ribbon lamellae crystallized at room temperature[18]. The crystal in *Figure 3a* has length of 0.75 μm and width of less than 0.2 μm. This can be compared with the ordinary long flat ribbons of polyDCHD, which have widths of 1 μm or more and lengths of hundreds of microns. The shape of this crystal is in the form of a short thin lamella with well-defined facets. The edges of the crystal are very straight, and make well-defined angles with each other. A selected area diffraction pattern taken from this crystal is shown in *Figure 3b*. It can be seen that the diffraction spots are arranged in an approximately hexagonal manner. Unlike SADP taken from a long ribbon polyDCHD, the diffraction spots of this pattern are very close and evenly spaced (the diffraction pattern is printed at the same magnification as the [1$\bar{1}$0] diffraction pattern). The diffraction pattern corresponds to a beam direction of [001], which means that the polymer chains in the crystal are oriented perpendicular to the carbon substrate and the lamellar surface. The indexed diffraction spots are shown next to the diffraction pattern. It is worth mentioning that the diffraction spots, particularly the 010 spot, in the [001] DP do not readily fade. This is understandable because all the spots correspond to *hk*0 planes which do not decay as rapidly as *hkl* spots[16]. The crystal face which is parallel to the plane of the substrate is (001) while the edges are determined as (010) (long edge) and (2$\bar{1}$0) (short edge). The morphology of this crystal is similar to that of conventional polymer single crystals such as polyethylene[28] in which the polymer chains are also oriented perpendicular to the lamellar surface. However, in the case of polyDCHD, there is no necessity for chain-folding on the lamellar surface. This is because the crystal is not grown by packing of long molecule chains, but by packing of individual monomer units stacking along the *c*-axis which link up to form polymer chains by solid-state polymerization.

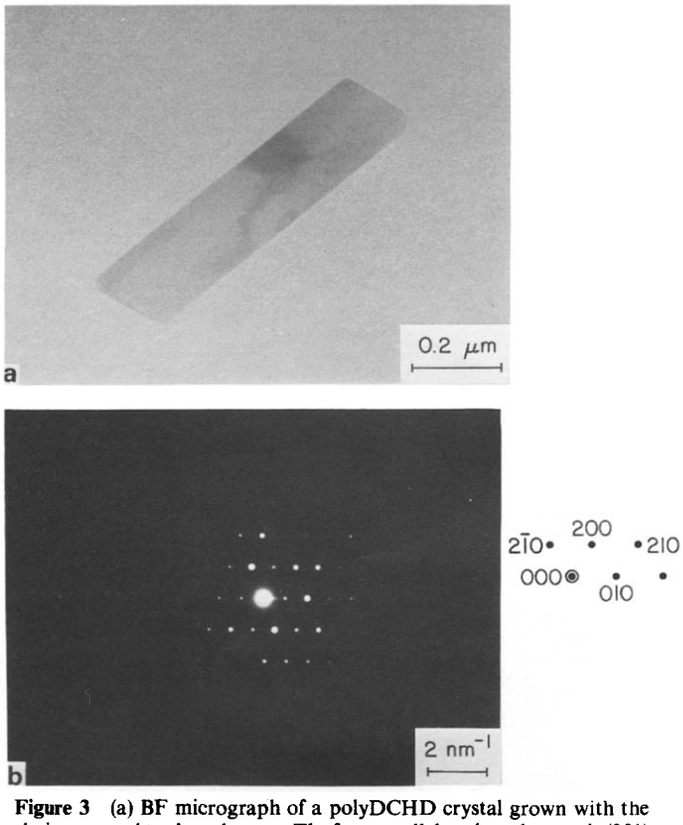

Figure 3 (a) BF micrograph of a polyDCHD crystal grown with the chains normal to the substrate. The face parallel to the substrate is (001) while the long and short edges correspond to (010) and (2$\bar{1}$0) faces respectively. (b) SADP of the end-on crystal in *Figure 3a*. The beam direction corresponds to [001]

The presence of these end-on crystals is thought to depend upon the rate of evaporation of the solvent. It is believed that DCHD crystals nucleate from the solution as small crystals similar to the one in *Figure 3a*. The crystals normally grow sideways and much faster along the *c*-axis. As the crystals grow longer along the *c*-axis, they become unstable and collapse with one of the facets lying parallel to the substrate. The crystals continue to grow until the solvent has evaporated, leaving the usual long ribbons of DCHD crystals lying on the substrate. The solution in the present case was, however, allowed to evaporate at 100°C so that the crystal growth rate may be much slower than the evaporation rate of the solvent. Some of the crystals were then prevented from growing any further so that the nuclei remained. Crystals of this type have an average thickness of about 30 nm as measured by a shadowing technique, although some thicker and more irregularly shaped end-on crystals were also found.

One- and two-dimensional lattice images

Figure 4 shows a high-resolution BF micrograph and SADP of an end-on polyDCHD crystal. The edges of the crystal in the micrograph were determined in the (010)

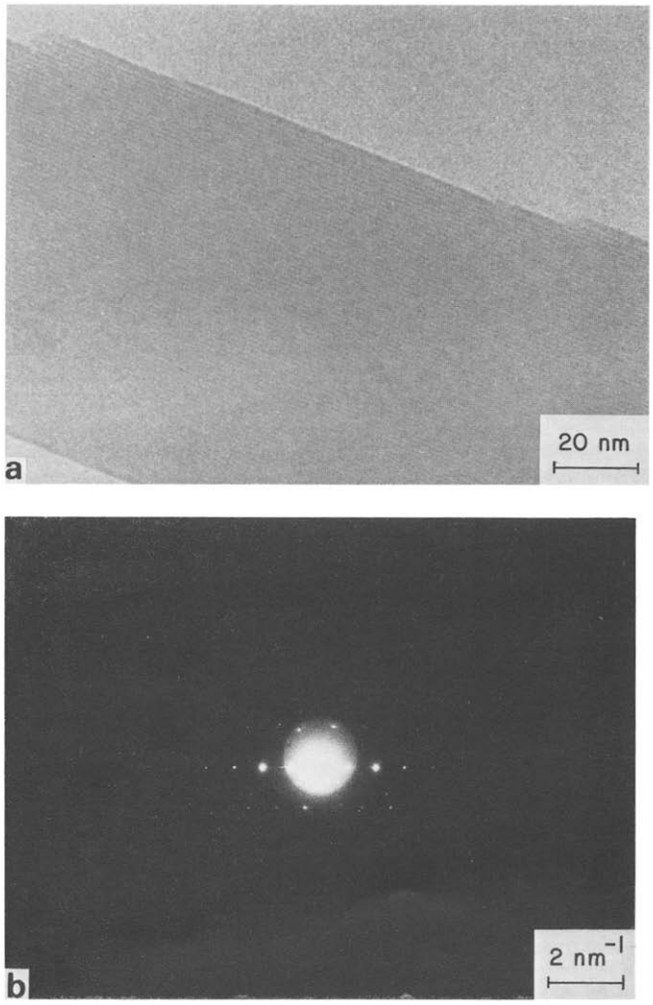

Figure 4 (a) (010) lattice image of end-on polyDCHD crystal. The lattice fringes can be seen terminated at the edge of minute steps. (b) [001] diffraction pattern of polyDCHD in *Figure 4a*. The doubly exposed area is the objective aperture used to enclose the diffraction spots

planes. It can be seen that the lattice fringes are parallel to the (010) edge. The fringes are very straight and parallel to each other and no disorder can be seen as in the side-on crystals. The spacing between the fringes was found to be 1.32 ± 0.1 nm, which is close to the d-spacing of (010) planes. It can also be seen from the micrograph that the crystal contains several small steps on the (010) facet, where lattice fringes are seen to terminate at the edges of these steps. The height of these steps ranges from a few lattice planes down to only one lattice plane. These small steps, which are probably involved in the monomer crystal growth process, are not easily seen at low magnifications and may also exist in the long ribbon crystals. As with the lattice images of the side-on crystals, this one-dimensional lattice contains little information about the position and shape of the molecules. It shows perfection of molecular packing of the (010) planes only but no information about other planes.

Figure 5a shows another high-resolution BF micrograph of part of an end-on polyDCHD crystal containing crossed-lattice fringes. It can be seen that one set of lattice fringes is running parallel to the (010) face while the other set is running parallel to the $(2\bar{1}0)$ face. The two sets of fringes cross each other to form a grid. The lattice spacing of the fringes running parallel to (010) face was found to be 1.33 ± 0.1 nm, which corresponds to the (010) lattice spacing. The other set of fringes has a spacing of 0.85 ± 0.05 nm. Since the fringes are parallel to the $(2\bar{1}0)$ face, have the same spacing as $(2\bar{1}0)$ planes and the angle between these fringes and (010) lattice fringes agrees with the calculated value (110.8°), they must correspond to $(2\bar{1}0)$ planes.

It is rather difficult to see whether or not the packing of the (010) and $(2\bar{1}0)$ planes is perfect in this crystal since the two sets of fringes cross each other and background noise is present. However, surface defects can still be seen in this crystal. A small step about one lattice plane thick can be seen on the (210) face. Structural images are still not to be expected because, as can be seen from the SADP in *Figure 5b*, the aperture (double-exposed area) enclosed only 16 diffraction spots, which is less than the number normally necessary (20) to form a full structural image from a suitably oriented crystal.

Molecular image of polyDCHD

Figure 6a shows a high-resolution BF micrograph of a part of a polyDCHD end-on crystal containing at least three sets of lattice fringes running in different directions and crossing each other in a relatively large area. The three sets of fringes that can be seen easily from the micrograph indicate very good lattice perfection. Fringes in each set are straight and parallel to each other. The fringes that have the widest spacing correspond to (010) planes. The other two sets of fringes have considerably smaller spacings and are found to be (210) and $(2\bar{1}0)$ planes. The measured d-spacings of the fringes and their

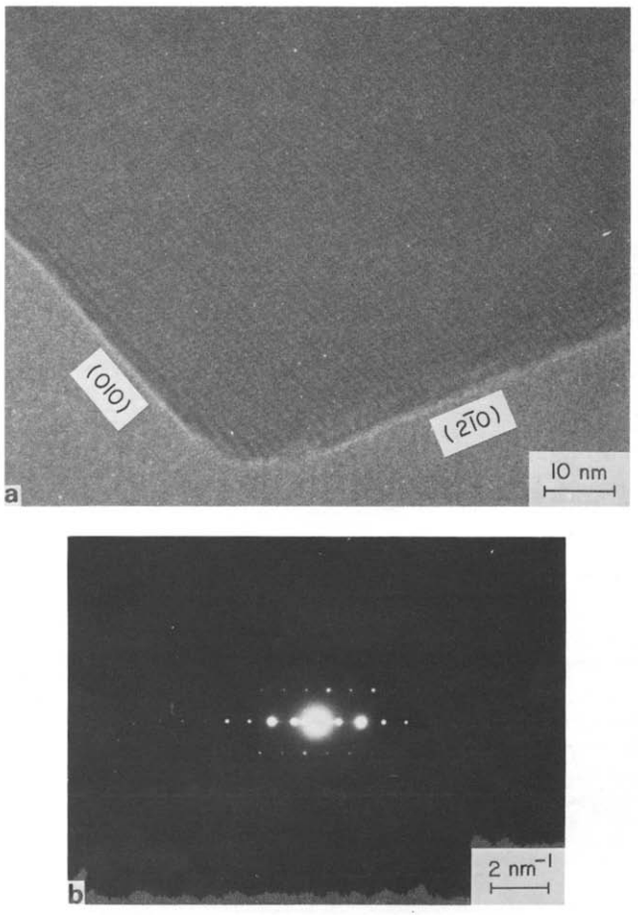

Figure 5 (a) Lattice images of an end-on polyDCHD crystal containing two sets of lattice fringes, (010) and $(2\bar{1}0)$. (b) SADP of the crystal in *Figure 5a*. The objective aperture enclosed 12 diffraction spots

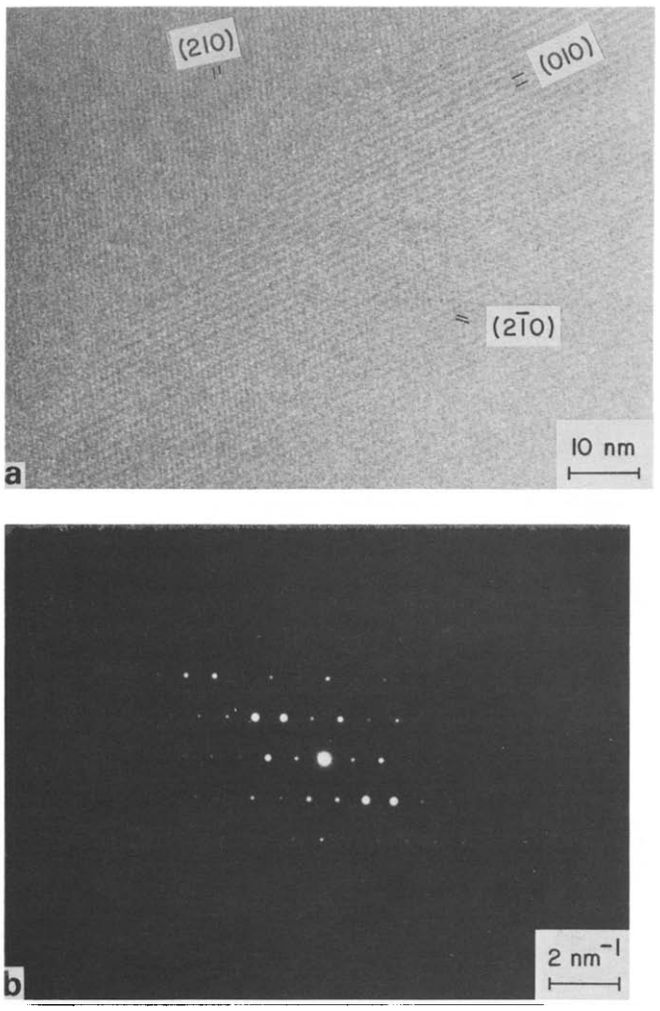

Figure 6 (a) Lattice image of part of a well oriented polyDCHD crystal showing 3 sets of lattice fringes crossing each other. (b) [001] diffraction pattern of the crystal in *Figure 6a*

Table 1 Comparison between the measured and calculated[a] *d*-spacings and interplanar angles of lattice fringes

	d-spacing (nm)		Angle with (010) (°)	
Lattice fringe	Measured	Calculated	Measured	Calculated
010	1.274	1.222	0	0
2$\bar{1}$0	0.832	0.813	69.5	69.13
210	0.614	0.602	44	43.8

[a] Calculations based on lattice constants determined by X-ray diffraction[26]

angles with (010) have been compared with calculated values based on X-ray determinations[26] and are summarized in *Table 1*. It can be seen from the Table that the measured and calculated values are very close. Although only three sets of lattice fringes are seen in the micrograph, lattice fringes corresponding to other planes with much smaller spacings may have been resolved, but they would be difficult to see at this magnification with the presence of background noise. The SADP of the crystal is shown in *Figure 6b*. The image was obtained using an objective aperture with a radius of about 3.2 nm^{-1} which enclosed at least 30 diffracted beams in contributing to the BF image. Under such conditions, the molecular image should be resolvable once the background noise is removed by filtering.

Image enhancement

Spatial averaging. Initial attempts to enhance the micrograph in *Figure 6a* involved the employment of the spatial averaging technique used by Fryer[5]. Although the background noise was reduced considerably, movement of the photographic paper was restricted to the three visible directions only. Any structural information that can only be revealed by movement in other crystallographic directions could not be obtained. The image enhanced using this method is shown in *Figure 7*. The image can be seen to have reduced background noise and the lattice fringes are more clearly seen running in three directions. In the area where the fringes are crossing each other, some small, individual dark patches can be seen. However, whether or not these patches represent the images of individual molecules cannot be ascertained as artefacts are sometimes produced by this technique. Nevertheless, it appears that the spatial averaging technique can produce significant improvement to the image.

Computer enhancement. The results of transforming the experimentally-obtained image to a computer enhanced image is shown in the series of pictures in *Figure 8*. In *Figure 8a*, a print of the experimental image was placed in front of the video camera linked to the DEC mini-computer. The diffraction pattern obtained by taking a Fourier transform of the image is shown in *Figure 8b*. It can be seen that the pattern contains five layers of bright discrete spots on a speckled background. There are 22 distinctive diffraction spots and although it is less than the number used to form the experimental image, it is more than the 20 necessary to form a structural image[20]. The apertures defined electronically around each spot are shown in *Figure 8c*. Finally, an image reformed from these spots with the background noise filtered can be seen in *Figure 8d*. This image contains individual dark patches in the shape of dumb-bells.

The vertical direction of the image in *Figure 8d* corresponds to the *a*-axis of the polymer crystal. The

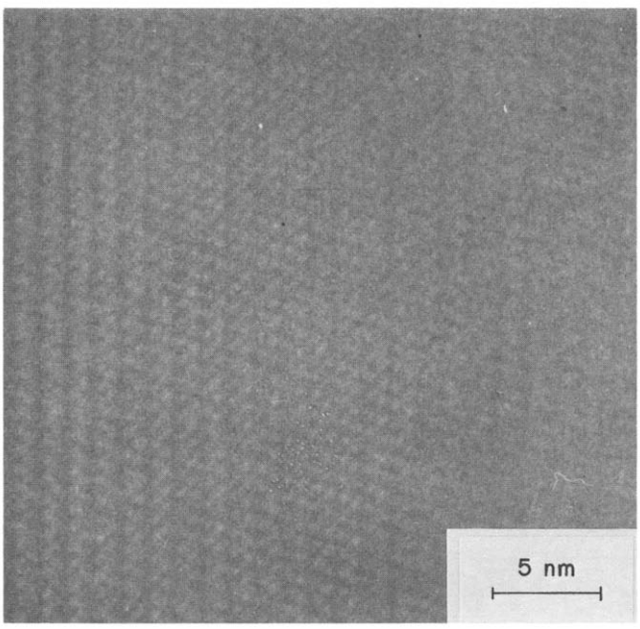

Figure 7 Molecular image of polyDCHD enhanced by the spatial averaging technique using *Figure 6a*. The fringes are seen clearly crossing each other and small dark patches are seen at the crossing points

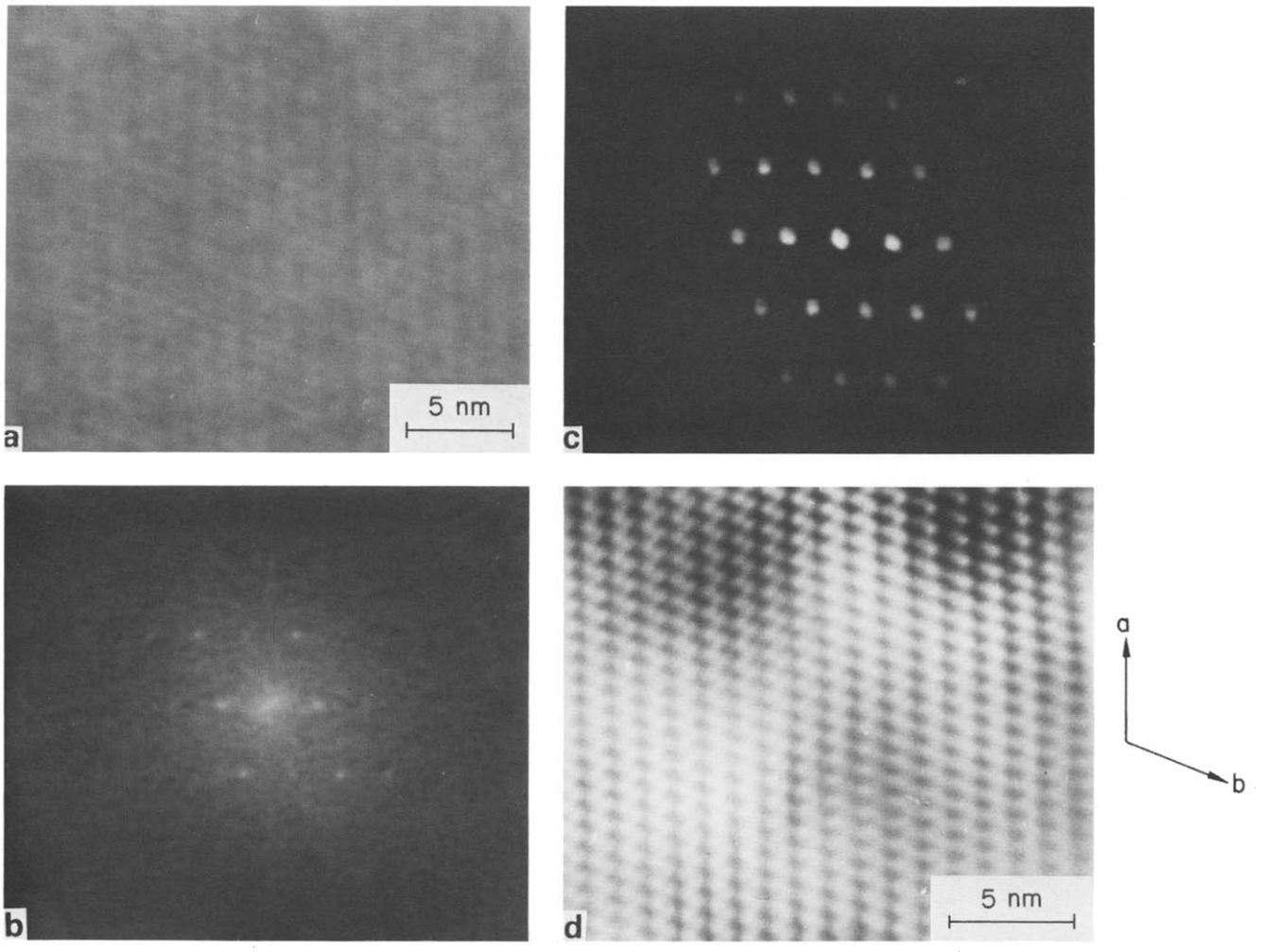

Figure 8 (a) Experimental molecular image of polyDCHD placed in front of video camera. (b) Diffraction pattern of the image in *Figure 8a*. There are 5 layers of discrete spots with a total of 22. (c) Diffraction pattern with apertures defined around each discrete spot. (d) Enhanced molecular image with the background noise removed. The vertical direction of the picture is the *a*-axis of the polymer

ratios between the spacings of some low index planes and their interplanar angles were measured from the enhanced image. These values were then compared with the calculated ones and the results are shown in *Tables 2* and *3*. It can be seen from the Tables that the agreement, particularly for the angles, between the measured and calculated values is very close. A few of the ratios between the interplanar spacings show a relatively large mismatch of up to 20%, which is probably due to distortions of the image as a result of multiple photographic processes and projection on the TV screen. The mismatch may also be due to film shrinkage and incorrect placement of the apertures on the diffraction pattern. Since the measured and calculated *d*-spacings and interplanar angles are in good agreement, each 'dumb-bell' is believed to be the image of an individual polyDCHC molecule viewed along the chain axis.

Computer simulation

The best way to ascertain that the experimental image represents the true image of the molecules is by comparison with computer simulated images such as those produced by n-beam dynamical calculations[29,30]. In the present study, calculations of polyDCHD molecular images were obtained using a similar method to that used by Jones[31]. The multi-slice theory of Cowley and Moodie[32] was used in calculating the images for

Table 2 Comparison between the ratios[a] of lattice planes spacings as measured from the enhanced image and calculated values[b]

	Measured ratios				
	(010)	(200)	(210)	(2$\bar{1}$0)	(220)
(200)	0.65	–	–	–	–
(210)	0.49	0.76	–	–	–
(2$\bar{1}$0)	0.63	0.98	1.29	–	–
(220)	0.36	0.56	0.73	0.57	–
(2$\bar{2}$0)	0.53	0.83	1.09	0.84	1.49

	Calculated ratios				
	(010)	(200)	(210)	(2$\bar{1}$0)	(220)
(200)	0.67	–	–	–	–
(210)	0.49	0.73	–	–	–
(2$\bar{1}$0)	0.66	0.98	1.35	–	–
(220)	0.35	0.52	0.71	0.53	–
(2$\bar{2}$0)	0.48	0.71	0.97	0.72	1.36

[a] The ratios are the spacings of the planes in the column divided by those in the row

[b] Calculations based on lattice constants determined by X-ray diffraction[26]

Table 3 Comparison between the interplanar angles as measured from the enhanced image and calculated values

Measured values (°)

	(010)	(200)	(210)	(2$\bar{1}$0)	(220)
(200)	107.2	–	–	–	–
(2$\bar{1}$0)	45	27	–	–	–
(210)	109.8	143	116	–	–
(220)	28.9	43	16.5	82	–
(2$\bar{2}$0)	135.2	63.7	90.8	25.2	74

Calculated values (°)

	(010)	(200)	(210)	(2$\bar{1}$0)	(220)
(200)	108.3	–	–	–	–
(2$\bar{1}$0)	43.8	27.9	–	–	–
(210)	110.9	140.8	112.9	–	–
(220)	29.7	42.0	14.1	81.2	–
(2$\bar{2}$0)	137.5	65.8	93.7	26.7	72.2

different crystal thickness. The thickness of each slice in the present case was taken as 0.5 nm. There are five programs in which crystallographic data of polyDCHD were imputed and the images were simulated and displayed on a computer monitor[31,33]. *Figure 9a* shows the projected potential for polyDCHD molecules on the *a–b* plane. It can be seen that the aromatic rings in the side groups and the projection of the backbone chain of the molecules form dumb-bell-shaped images. This is a perfect image that cannot be obtained in a microscope. The image in *Figure 9b* was calculated for a particular C_s value, crystal thickness, defocus value etc. It must be stressed that the shape of the simulated images is sensitive to changes in any of the input parameters, especially the value of defocus. The simulated image in *Figure 9b* can also be seen to exhibit columns of 'dumb-bells' which are similar to the experimental image. Although the crystal thickness and value of defocus in this case are not certain due to the low level of beam intensity employed and the lack of specimen contrast, since the calculated image has a similar C_s value as the experimental image, and the objective aperture sizes used to form the images are similar, the two images may be compared with each other as shown in *Figure 10*. The fact that the features in the images agree well helps to prove that the experimental image is that of polyDCHD molecules viewed along the *c*-axis. This has also confirmed the crystal structure of polyDCHD determined by other workers[14,26]. It can also be seen from the experimental image that, in the area viewed, there is no disorder in the packing of the molecules, which means that the area is completely defect free. It has also confirmed that the molecules are all lying perpendicular to the surface of the lamellar crystal so that the images of backbone chains and side groups can be obtained.

CONCLUSIONS

Lattice images covering large areas of a polyDCHD crystals lying with the chains parallel to the substrate have been obtained using high-resolution electron microscopy and these images are similar to those obtained by other workers[16,17]. It has also been shown that lattice images from planes other than (*hk*0) can be resolved and images of

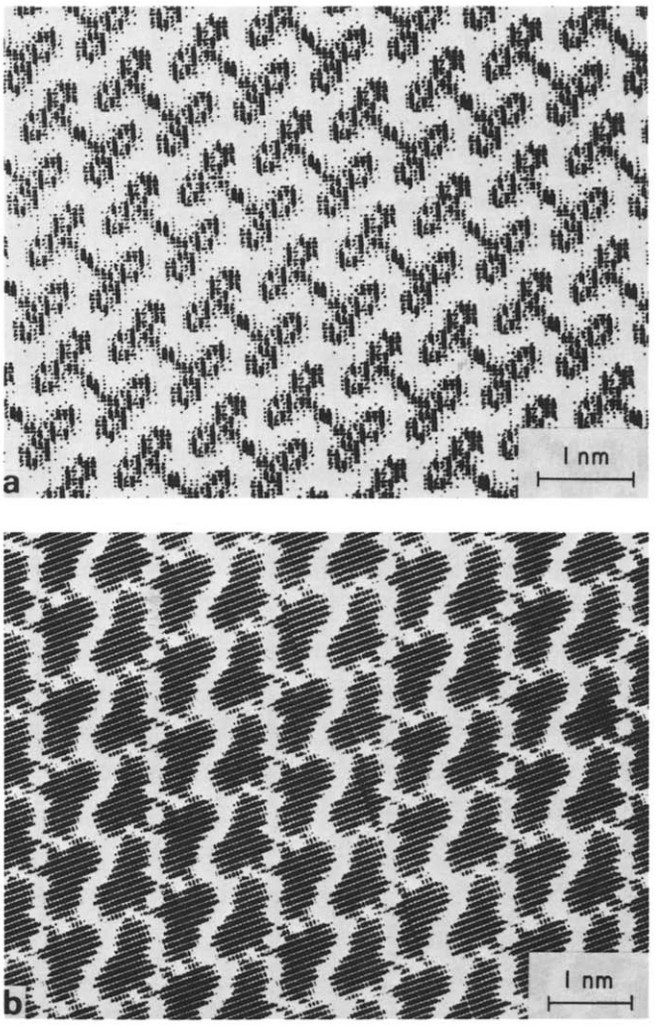

Figure 9 (a) Projection of polyDCHD molecules on *a–b* plane. (b) Computer simulated polyDCHD molecules viewed along the molecular axis. The image forming parameters are similar to those of the experimental image.

C_s (spherical aberration constant) = 1.2 mm;
r (objective aperture radius) = 4 nm^{-1};
θ_c (beam divergence) = 0.3 mrad;
Δ (chromatic focus spread) = 25 nm;
Δ_f (defocus value) = −65 nm;
t (specimen thickness) = 15 nm

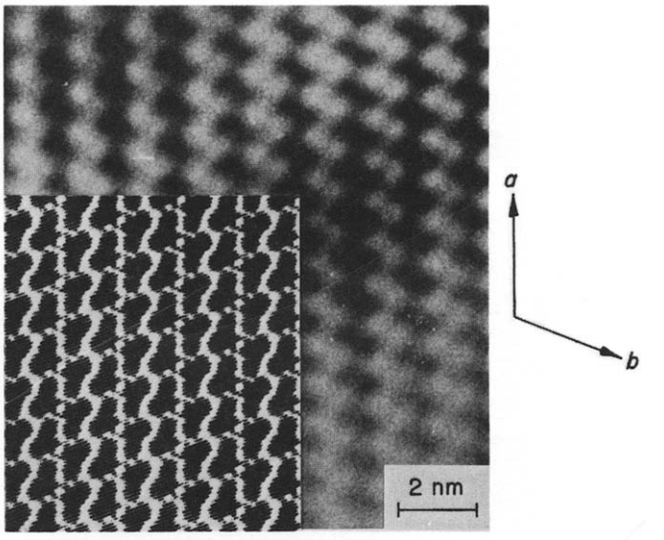

Figure 10 Comparison between the experimental enhanced image of polyDCHD molecules with computer simulated image

(*hkl*) lattice planes have been obtained for the first time in polyDCHD.

Crystals of polyDCHD with a different orientation have been obtained using a new specimen preparation method. The crystals are lamellar with the chains oriented perpendicular to the substrate. Such crystals have allowed lattice and molecular images to be obtained with the electron beam parallel to the chain axis. An enhanced experimental image has been compared with computer simulated images. Features in the enhanced image are found to resemble the calculated dumb-bell-shaped images of polyDCHD molecules viewed along the molecular axis. This is the first time that molecular images of a diacetylene polymer have been obtained and the images have confirmed the crystal structure determined by other workers.

ACKNOWLEDGEMENTS

This work was supported by the US Army through its European Research Office. The authors wish to thank Prof D. Bloor of the Physics Department and Dr C. Gallotis of the Materials Department, Queen Mary College, for supplying the diacetylene monomer. They would also like to thank Dr M. J. Goringe and Dr C. J. Humphreys of the Department of Metallurgy and Science of Materials, University of Oxford, for the help with image enhancement and image simulation respectively.

REFERENCES

1 Hashimoto, H., Endoh, H., Takai, Y., Tomioka, H. and Yokota, Y. *Chem. Scrip.* 1979, **14**, 23
2 Cosslett, V. E., Camps, R. A., Saxton, W. O., Smith, D. T., Nixon, W. C., Ahmed, H., Catto, C. J. D., Cleaver, J. R. A., Smith, K. C. A., Timbs, A. E., Turner, P. W. and Ross, P. M. *Nature* 1979, **281**, 49
3 Anderson, J. S. *Chem. Scrip.* 1979, **14**, 129
4 Murata, Y., Fryer, J. R. and Baird, T. *J. Micro.* 1976, **108**, 261
5 Fryer, J. R. *Acta Cryst.* 1978, **A34**, 603
6 Dobb, M. G., Johnson, D. J. and Saville, B. P. *J. Polym. Sci., Polym. Symp.* 1977, **58**, 237
7 Shimamura, K., Minter, J. R. and Thomas, E. L. *J. Mater. Sci., Lett.* 1983, **2**, 54
8 Uyeda, N., Kobayashi, T., Suito, E., Harada, Y. and Watanabe, M. *J. Appl. Phys.* 1972, **43**, 5181
9 Uyeda, N., Kobayashi, T., Ishizuke, K. and Fujiyoshi, Y. *Chem. Scrip.* 1979, **14**, 47
10 Dobb, M. G., Hindeleh, A. M., Johnson, D. J. and Saville, B. P. *Nature* 1975, **253**, 189
11 Bassett, G. A. and Keller, A. A. *Kolloid-Z.* 1969, **231**, 386
12 Tsuji, M., Isoda, S., Ohara, M., Kawaguchi, A. and Katayama, K. *Polymer* 1982, **23**, 1568
13 Isoda, S., Tsuji, M., Ohara, M., Kawaguchi, A. and Katayama, K. *Polymer* 1983, **24**, 1155
14 Enkelmann, V., Leyner, R. J., Schleier, G. and Wegner, G. *J. Mater. Sci.* 1980, **15**, 168
15 Yee, Y. C. and Chance, R. R. *J. Polym. Sci., Polym. Phys. Edn.* 1978, **16**, 431
16 Read, R. T. and Young, R. J. *J. Mater. Sci.* 1984, **19**, 327
17 Read, R. T. and Young, R. J. *J. Mater. Sci.* 1981, **16**, 2922
18 Galiotis, C., Read, R. T., Yeung, P. H. J., Young, R. J., Chalmers, I. F. and Bloor, D. *J. Polym. Sci., Polym. Phys. Edn.* 1984, **22**, 1589
19 Yeung, P. H. J. PhD Thesis, University of London, UK, 1984
20 Spence, J. C. H. in 'Experimental High-Resolution Electron Microscopy', Clarendon Press, Oxford, UK, 1981
21 Glaeser, R. M. in 'Physical Aspects of Electron Microscopy Microbeam Analysis', (Ed. B. Biegel and D. R. Beaman), John Wiley, New York, USA, 1975, p. 205
22 Unwin, N. and Henderson, R. *Scientific American*, 1984, Feb., 56
23 Klug, A. and DeRosier, D. J. *Nature* 1966, **212**, 29
24 Crowther, R. A. and Klug, A. *Annual Rev. Biochem.* 1975, **44**, 878
25 Boyes, E. D., Goringe, M. J., Gill, J. J., Muggridge, B. J., Northover, J. P. and Salter, C. J. *Inst. Phys. Conf. Ser.* 1983, **68**, 211
26 Apgar, P. A. and Yee, K. C. *Acta Cryst.* 1978, **B34**, 957
27 Grubb, D. T. *J. Mater. Sci.* 1974, **9**, 1715
28 Keller, A. *Phil. Mag.* 1957, **2**, 1171
29 Lynch, D. F. and O'Keefe, M. A. *Acta Cryst.* 1972, **A28**, 536
30 O'Keefe, M. A. *Acta Cryst.* 1973, **A29**, 389
31 Jones, J. C. *J. Mater. Sci.* 1984, **19**, 533
32 Cowley, J. M. and Moodie, A. F. *Proc. Phys. Soc.* 1960, **76**, 378
33 Skarnulis, A. J. *J. Appl. Cryst.* 1979, **12**, 636